

Satellite Tracking and Characterization Using Signal Data

Principal Author: David Richmond

Lockheed Martin

Co-Author: Tatum Poole

Lockheed Martin

CONFERENCE PAPER

1. ABSTRACT SUMMARY

Our team evaluated an approach for determining the radial velocity and position of a satellite using the downlink signal quality and computing an azimuth and elevation offset bias. This approach is derived in this paper. We conducted a comparison of this approach with the work our team did last year for evaluating the Doppler frequency shift of satellite signals observed by a user on the ground as a function of time to determine the radial velocity and position of the satellite using the Doppler frequency shift. This comparison is presented to include antenna calibration requirements, ability to track unknown objects, and expected accuracy for each of four orbital types: LEO, MEO, GEO and Inclined GEO. The benefits of such information are discussed, to include alternative catalog maintenance sensor, maneuver tip and queue, and anomaly resolution support. Conclusions regarding the two approaches are provided.

2. INTRODUCTION

The ability to determine the current position and velocity and to predict the future position of satellites (metric data) has been a need ever since the first objects were launched into orbit. The initial Space Surveillance Network (SSN) was comprised of a network of phased array radar sensors, many of which had a primary mission other than tracking satellites. When satellites began to utilize geosynchronous orbits (GEO), optical telescopes were added to the SSN to augment the phased array space tracking capabilities. The methods used to identify the observed object rely heavily on the object's actual position with respect to the object's expected position. Errors in the expected position have caused misidentification, resulting in cross-tagging objects. Occasionally, objects may not be located at all because of maneuvers resulting in their placement on the lost list. These issues are more severe in the GEO regime due to the inability of ground-based sensors to produce resolved images.

In recent years, the term "space surveillance" has been subsumed by the broader term "space domain awareness," which adds additional types of information to metric data with the goal of characterizing objects in space as well as the space environment itself. *Comparison of Phenomenology for Satellite Characterization* [1] identified satellite characteristics and mapped them phenomenology. Techniques of determining characteristics of on orbit objects was introduced in *Satellite Characterization Data Collection and Analysis* [2]. In this paper, our focus is the Radio Frequency (RF) signal produced by the satellite and a comparison of two algorithms used to provide the characteristics.

To collect signal information from an object of interest, an antenna is required. A typical antenna installation supports a specific operational system and is not available to be tasked for general passive collections. However, our research team in Valley Forge, PA obtained a decommissioned S-band Phased Array antenna that was still in operable condition. The antenna has been installed at our research site in Valley Forge to perform passive data collects of S-band signals from LEO, MEO and GEO regimes.

The Phased Array antenna provides a 60-degree field of view in the east-west direction as depicted in Figure 1. It consists of two 9'x8' panels, each providing 3 beams with 8 dB/K of gain. Alternatively, each panel can provide 6 beams with 5 dB/K of gain by leveraging a Phased Array antenna technique known as "beam partitioning." The electronically-steered array is capable of monitoring position and velocity of target objects, rapidly identifying when a maneuver has been performed by detecting gain fluctuations, geo-locating ground transmitters, and identifying electro-magnetic interference (EMI).

Phased Array Antenna

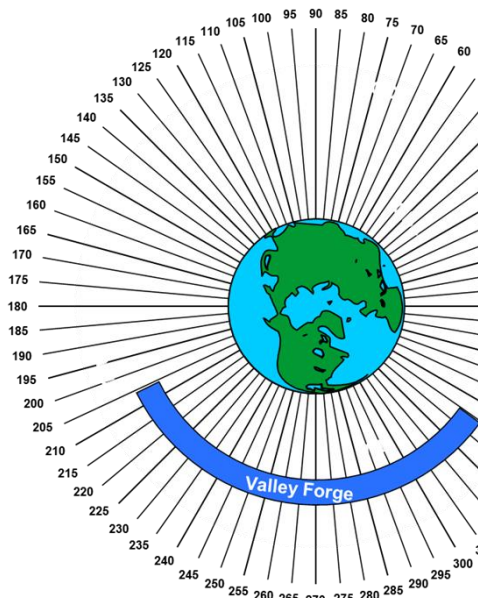


Figure 1: Phased Array Antenna

3. DOPPLER TRACKING

Observation of the Doppler frequency shift during a satellite pass can provide sufficient information for accurate orbit determination. Velocity determination has been seen using Doppler shift measurements through a closed-form ECEF satellite acceleration formula derived from the rotation matrix method described in *GPS Satellite Velocity and Acceleration Determination using the Broadcast Ephemeris* [3].

LEO's have been used in finding orbit and Doppler calculations that are used to derive general orbital models described in *Orbit Calculation and Doppler Correction Algorithm in a LEO Satellite Small Ground Terminal* [4]. Doppler-aided velocity and position algorithms have been determined, but not to the point where they are used to form more accurate orbital determinations while actively tracking is described in *Carrier Phase & Doppler-Based Algorithms for Real-Time Standalone Positioning* [5].

During the transit of a satellite in low earth orbit, the received signal frequency will typically vary from several thousand Hz above, to several thousand Hz below the transmitter frequency. Figure 2 shows a representative variation of frequency with time for a high inclination orbit, where the center frequency is 2245.673 MHz.

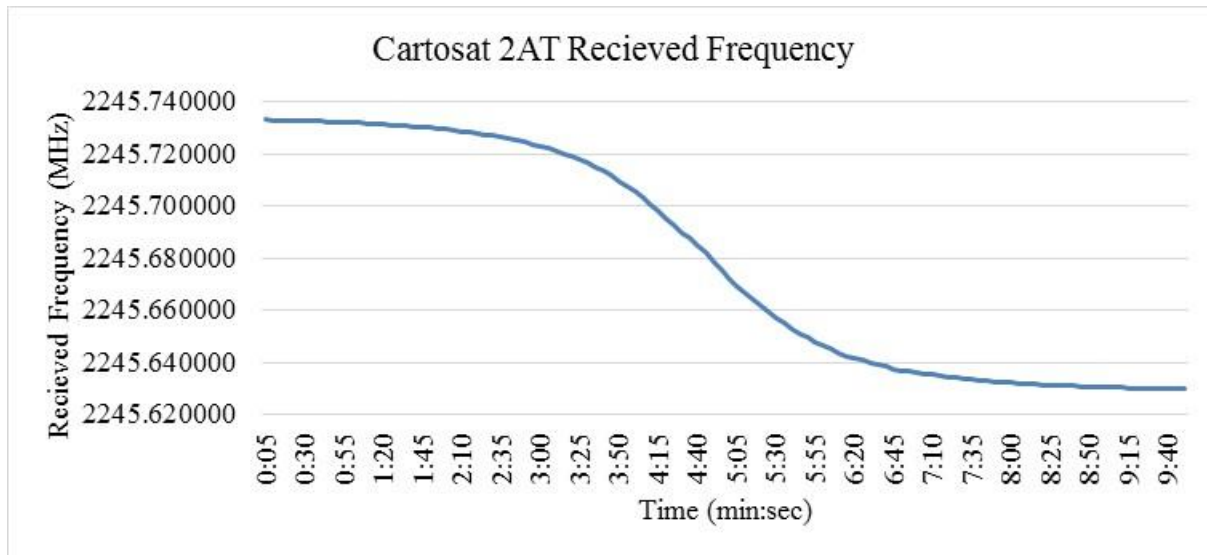


Figure 2: Graph of the received frequencies during an overhead pass of the Cartosat 2AT satellite from a location in Valley Forge, PA on the 6th of April 2018

The Doppler curve is a function of the relative motion between the receiving site and the satellite. Given the ground station coordinates are well determined, the only unknown components of the relative motion are due to the motion of the satellite, and the curve is solvable for the orbit. Conversely, if the satellite orbit is well determined, the location of the receiving station can be determined, and the satellite becomes useful for navigation. From this information our team derived the position and velocity as described in *Doppler Curves in Satellite Tracking and Characterization* [6].

4. SIGNAL QUALITY TRACKING

Unlike traditional monopulse multimode tracking feeds (i.e., TE11 & TM01 mode comparison), a phased array antenna can perform autotracking using downlink signal quality estimates with known azimuth and elevation offsets to calculate an Az/El correction bias. This is commonly referred to as a spiral scan or a conical scan.

Downlink Signal Quality

For a phased array, the algorithm requires a signal quality estimate (e.g. C/No, Eb/No, Es/No), which will include power fluctuations from atmospheric effects (e.g. scintillation, varying rain rates, varying clouds). The performance of the algorithm is dependent upon these fluctuations because the magnitude will impact the proposed azimuth and elevation offsets.

Antenna Autotracking

A Gaussian approximation is commonly used to predict the pointing loss from antenna pointing error. Figure 3 shows a projection view (left) and top down view (right) of the normalized antenna gain as a function of azimuth and elevation offsets normalized by the half power full beamwidth (θ_{3dB}).

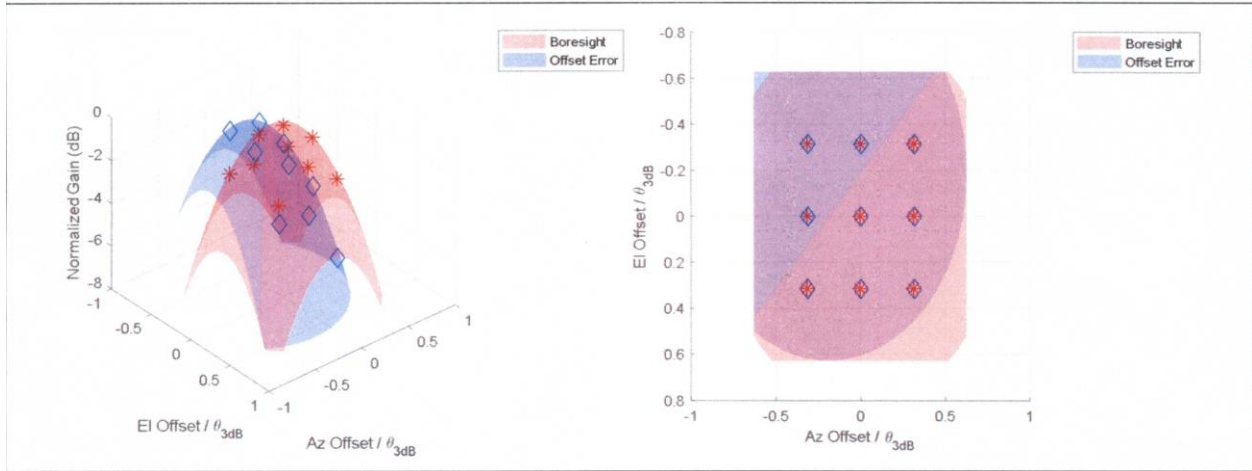


Figure 3: Projection view (left) and top down view (right) of the normalized antenna gain as a function of azimuth and elevation offsets

For circular phased arrays, the normalized gain above follows the Gaussian approximation of the Bessel function of the first kind order one as shown in Eq (1). For rectangular phased arrays the same Gaussian approximate can be utilized.

$$\Delta G(\theta_{AZ}, \theta_{El}) \approx -12 \cdot \frac{\theta_{AZ}^2 + \theta_{El}^2}{\theta_{3dB}^2} \quad (1)$$

Figure 4 shows the differences between the normalized gain or pointing loss for a sinc function (i.e., rectangular arrays), a Bessel function of the first kind order one (i.e. circular arrays), and the approximation in Eq. (1) derived from a Gaussian approximation.

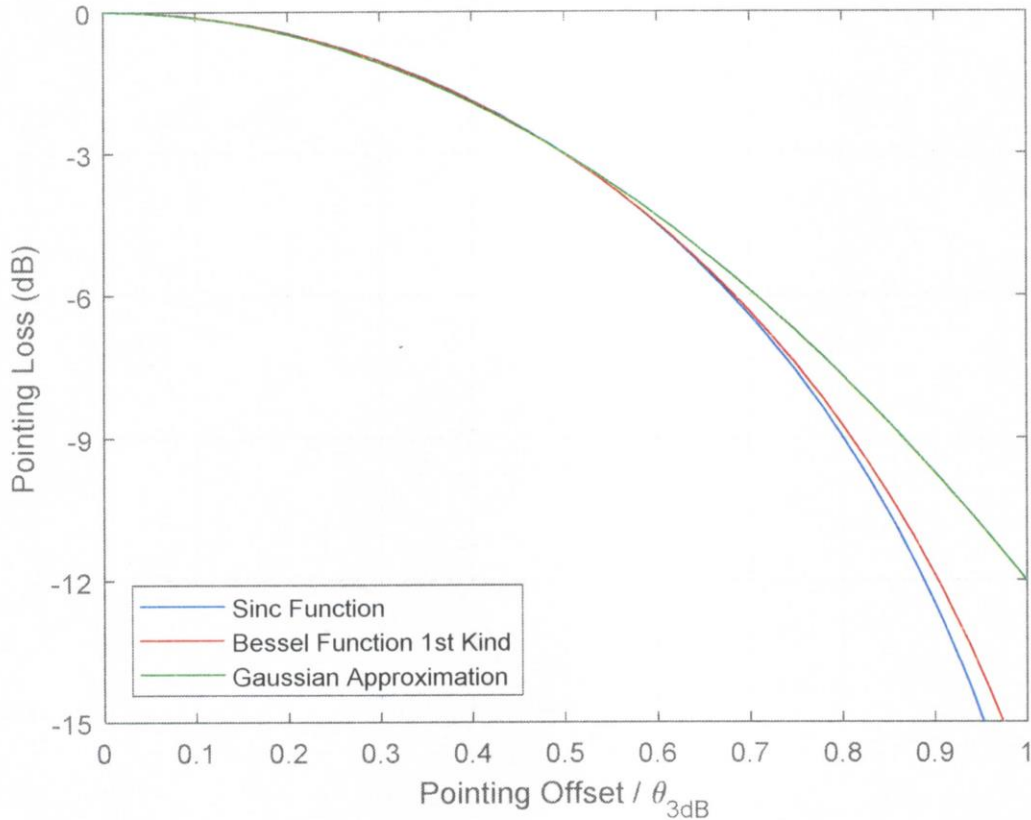


Figure 4: Comparison of antenna pointing loss with Gaussian approximation

For the “boresight” paraboloid shown as red in Figure 3, the normalized gain measurements (i.e., red stars) will be symmetric. For example, the center point would be the maximum (i.e., $\Delta G(0, 0)=0$), The midpoints along the edges would be reduced (i.e., $\Delta G(\pm\theta_{Az}, 0) = \Delta G(0, \pm\theta_{El}) = -\Delta$), and the corner points would be reduced by two times (i.e., $\Delta G(\pm\theta_{Az}, \pm\theta_{El}) = -2\Delta$).

For the “offset error” paraboloid shown as blue in Figure 3, the normalized gain measurements (i.e. blue diamonds) would not be symmetric with pointing errors, but these measurements would still follow Eq. (1).

For the simple case when neglecting noise, the difference between “offset error” paraboloid measurements ($C/N_{o_{measured}}(\theta_{Az}, \theta_{El})$ in units of dBHz) and “boresight” paraboloid values ($\Delta G(\theta_{Az}, \theta_{El})$ in units of dB) will result in data points ($C/N_{o_{corr}}(\theta_{Az}, \theta_{El})$ in units of dBHz) that lie on a plane having a tilt that is proportional to Az,El correction bias as shown in Eq. (2).

$$C/N_{o_{corr}}(\theta_{Az}, \theta_{El}) = C/N_{o_{measured}}(\theta_{Az}, \theta_{El}) - \Delta G(\theta_{Az}, \theta_{El}) \quad (2)$$

When accounting for noise, the resulting data points ($C/N_{o_{corr}}(\theta_{Az}, \theta_{El})$ in units of dBHz) will not lie on a plane, but Singular-Value Decomposition (SVD) is used to determine the “best fit” plane from multiple data points (i.e., M is an $N \times 3$ matrix of $(\theta_{Az}, \theta_{El}, C/N_{o_{corr}}(\theta_{Az}, \theta_{El}))$ where N is the number of data points). From SVD factorization of the matrix, U is the $N \times N$ matrix of left-singular vectors, Σ is the $N \times 3$ diagonal matrix of singular values, and V^T is the 3×3 matrix of right-singular vectors. Note prior to performing SVD factorization, the matrix M should be centered (i.e., subtracting the column mean from each column value).

$$\mathbf{M} = \begin{bmatrix} \theta_{Az_1} & \theta_{El_1} & C/No_{corr_1} \\ \theta_{Az_2} & \theta_{El_2} & C/No_{corr_2} \\ \vdots & \vdots & \vdots \\ \vdots & \vdots & \vdots \\ \theta_{Az_N} & \theta_{El_N} & \theta_{El_N} C/No_{corr_N} \end{bmatrix} = \mathbf{U} \mathbf{\Sigma} \mathbf{V}^T \quad (3)$$

For the Nx3 singular value matrix (Σ), the ratio of the last two singular values ($\Sigma_{33} / \Sigma_{22}$) in Eq. (4) provides Scoring Metric for the “goodness” of the plane fit. Specifically, when $\Sigma_{33} / \Sigma_{22}$ is greater than 0.75, any calculated Az/El correction bias should be ignored because the matrix of data points (\mathbf{M}) may be insufficiently coplanar.

$$\mathbf{\Sigma} = \begin{bmatrix} \Sigma_{11} & 0 & 0 \\ 0 & \Sigma_{22} & 0 \\ 0 & 0 & \Sigma_{33} \end{bmatrix} \quad (4)$$

For the 3x3 matrix of right-singular vectors (\mathbf{V}), the third column (V_{13} in units of deg^{-1} , V_{23} in units of deg^{-1} , V_{33} in units of $dBHz^{-1}$) provides the normal vector of the “best fit” plane in Eq. (5).

$$\mathbf{V} = \begin{bmatrix} V_{11} & V_{12} & V_{13} \\ V_{21} & V_{22} & V_{23} \\ V_{31} & V_{32} & V_{33} \end{bmatrix} \quad (5)$$

Finally, the Az, El correction bias is calculated from the normal vector of the “best fit” plane and antenna paraboloid scaling using Eq. (6) and (7). Note the equations below assume that the azimuth and elevation full 3dB beamwidths are equivalent, but this is not required.

$$Az = \frac{V_{13}}{V_{33}} \cdot \frac{\theta_{3dB}^2}{2 \cdot 12} \quad (6)$$

$$El = \frac{V_{23}}{V_{33}} \cdot \frac{\theta_{3dB}^2}{2 \cdot 12} \quad (7)$$

Implementation

Based on the half power beamwidth from the phased array and signal quality (e.g., C/No, Eb/No, Es/No), an optimization should be performed to select the spiral/conical scan rate, azimuth and elevation offset magnitude, and number of points for averaging (N) with a limiting constraint being the $\Sigma_{33} / \Sigma_{22}$ ratio for “goodness” of the plane fitting the data (i.e., smaller is better).

5. COMPARISON

Antenna Calibration Requirements

Doppler tracking is not dependent on the pointing accuracy of the antenna. The antenna simply needs to be accurate enough to collect a signal from the desired object. The Doppler Tracking approach is dependent upon the accuracy of the measured signal strength and the accuracy of the time value assigned to these measurements. Our time source comes from GPS time. The measurements are recorded using a software defined radio (SDR).

Signal Quality tracking produces a pointing bias from the expected Azimuth/Elevation values. Proper calibration of the pointing accuracy of the antenna results in improved position accuracy. The azimuth accuracy is calibrated by identifying north entering any azimuth offset based on true north. The elevation calibration is dependent upon proper leveling of the mount structure.

Unknown Object Track

Doppler tracking can establish position estimates for unknown objects. This is accomplished by pointing the antenna at a specific location and recording the signal as the object passes through the antenna field of view. Post pass processing based on an estimated transmit frequency can be used to perform an initial orbit determination. This initial orbit determination is used to identify a second pass to collect again. Collecting the entire second pass provides enough data to identify the transmit frequency of the object and then Doppler shifts over the entire pass can be identified.

Signal Quality tracking approach requires an estimate of the orbit to determine an Az/EI bias. Thus, with no other data this approach is not able to track unknown objects. However, this approach can be combined with the initial orbit determination obtained using the Doppler information to refine the orbital elements.

Expected Accuracy

Doppler tracking using a single receiver produced adequate results for LEO objects. As the objects moved further away (i.e. MEO and GEO) the relative velocity became smaller. This small relative velocity made measuring Doppler changes more difficult for MEO and GEO objects causing the accuracy to degrade.

Signal Quality tracking approach produces very accurate results. This accuracy did not degrade based on orbital type.

6. BENEFITS

Passive collecting signals as an alternative catalog maintenance sensor provides additional information such as the downlink signal to confirm the observed object is the expected object. Having this additional information reduces the misidentification that results in cross-tagging objects. Observing the downlink signal of an unknown object or identification of a maneuver of a known object can be used to tip and queue other sensors.

7. CONCLUSION

We are in the early stages of our research. We have established a set of desired satellite attributes that can be derived using an antenna that passively receives signals transmitted from on orbit objects. Our current effort verified that position and velocity can be determined for multiple orbital regimes. Additionally, maneuvers can be identified as unexpected changes in the velocity. Our goal going forward is to evaluate approaches to improve the accuracy of the measurements and understand the residuals. Longer term we would establish a historical database for all objects to establish pattern of life baselines.

8. REFERENCES

1. Richmond, D., Spoto, G., “*Comparison of Phenomenology for Satellite Characterization*”, Proceeding of AMOS 2016 Technical Conference.
2. Richmond, D., and Brennan, J., “*Satellite Characterization Data Collection and Analysis*”, Proceeding of AMOS 2017 Technical Conference.
3. Zhang, J., Zhang, K., Grenfell, R., and Deakin, R., “*GPS Satellite Velocity and Acceleration Determination using the Broadcast Ephemeris*”, The Journal of Navigation (2006), **59**, 293-305.
4. Zantou, E. B., Kherras, A., and Addaim, A., “*Orbit Calculation and Doppler Correction Algorithm in a LEO Satellite Small Ground Terminal*”, Proceeding of 19th Annual AIAA/USU Conference on Small Satellites.
5. Simsky, A., and Boon, F., “*Carrier Phase & Doppler-Based Algorithms for Real-Time Standalone Positioning*”, Septentrio NV, Belgium (2003).
6. Richmond, D., and Brennan, J., “*Doppler Curves in Satellite Tracking and Characterization*”, Proceeding of AMOS 2018 Technical Conference.